RETROFIT OF HYDROGEN-POWERED HELICOPTERS: AN OPTIMAL APPROACH

Andrea Nesci[1], Giorgio Vicenzotti[2], Massimo Brunetti[2] and Francesco Salucci[1]

[1] Chief Technology and Innovation Office, Leonardo Labs, Leonardo S.p.A.
andrea.nesci.ext@leonardo.com / francesco.salucci.ext@leonardo.com
[2] Research and Innovation Office, Leonardo Helicopters Division, Leonardo S.p.A.
massimo.brunetti@leonardo.com / giorgio.vicenzotti@leonardo.com

ABSTRACT

In the framework of developing a climate-neutral aviation industry, hydrogen could play a critical role in the future. Given hydrogen's high specific energy but fuel cells' low specific power, this technology can be effectively used in conjunction with batteries, which have opposing characteristics. To that end, it is critical to develop design methodologies that allow for effective component integration and weight optimization. Therefore, this article introduces an original algorithm, HERACLES, which solves a constrained non linear optimization problem, aiming to find the lightest hydrogen-driven powertrain able to replace the conventional thermal engine-driven powertrain of a generic rotorcraft, preserving its given Maximum Take Off Weight (MTOW) and airframe. In order to demonstrate the effectiveness of the methodology, this is applied to a reference helicopter representative of the heavy category, MTOW of about 9 ton, considering a FC-based architecture. The optimal results are presented and then compared to a first sizing guess, showing the improvements on the payload obtainable with a better system integration. Finally, some sensitivity studies are carried out to picture the impact of the main technological key performance indexes on aircraft payload.

NOMENCLATURE

Symbols

ϕ	Hybridization factor	-
τ	Torque	Nm
Ω	Rotational speed	rad/s
$J(\boldsymbol{x})$	Cost function	-
M	Mass	kg
N	Number of samples	-
n	Number of modules	-
P	Power	W
$\boldsymbol{x}$	Optimization vector	-

Subscripts

0	Normalization factor
B	Battery
C	Cables
GB	Gearbox
H_2	Hydrogen
T	Tank

Acronyms

BoP	Balance of Plant
EM	Electric Motor
eVTOL	electric Vertical Take-off and Landing
FC	Fuel Cell
MTOW	Maximum Take Off Weight
OEI	One Engine Inoperative
PEM	Proton Exchange Membrane
ROHGER	Retrofit Of HydroGen powEred Rotorcraft
SoC	State of Charge
TE	Thermal Engine
TEH-R	Twin Engine Heavy Helicopter 2020 Reference
TMS	Thermal Management System

1 INTRODUCTION

Recently, the interest in electric Vertical Take-off and Landing (eVTOL) aircraft has enormously increased as proved by the exponential growth of publications [1] and by the number of existing eVTOL aircraft designs [2]. A crucial limiting factor for the development of an electrical propulsion based aviation is related to the low energy density of current batteries which conversely have reached good performance in power density [3]. Therefore, a powertrain which combines power specialized lithium-ion cells with high specific energy hydrogen-powered Proton Exchange Membrane (PEM) Fuel Cells (FCs) could take advantage of both technologies: extend the aircraft range and provide a suitable maneuvering capability [4]. However, although the advantages of a battery-FC powertrain have been already proved for fixed-wing aircraft [5]–[8], rotorcraft requirements pose unique challenges: VTOL and hover capabilities necessitates higher power-to-weight ratios while the large hydrogen tanks more volume [9], [10].

In this paper, we present an original methodology, HERACLES, which can optimize any hydrogen-driven powertrain, aiming to maximize the total payload of the aircraft for a datum MTOW, while preserving the original flight performance and which is here applied to a FC hybrid-electric powertrain architecture. Furthermore, the proposed methodology generates a battery and a FC optimal power profile, specific for the considered flight mission, which ensures that the battery has always an adequate State of Charge (SoC), even in the event of an emergency. Moreover, the optimized powertrain complies with the safety constraints related to the One Engine Inoperative (OEI) condition: the FC and the battery packs are partitioned into a number of modules, which ensures that the total required power can be delivered even in case of a certain number of failures. Actually, a number of optimization-based design approaches [11], [12], including an energy management algorithm for the minimization of hydrogen consumption over nominal mission profiles [13], have made significant contributions to the proposed solution. Results refer to a rotorcraft demonstrator based on 2020 state-of-art and a series hybrid powertrain architecture.

This paper further demonstrates the capability of this methodology through a number of sensitivity analyses, useful to evaluate how the hybridization factor and payload change with the assumptions on FC, battery and tank technological state of the art. This allows for several considerations concerning the potential for hydrogen-powered VTOL aircraft in light of ongoing advancements in FC and battery technology.

2 METHODOLOGY

The ability of sizing a hydrogen-driven powertrain for a given aircraft with a given MTOW and airframe represents a fundamental element in drafting study cases and retrofit exercises to investigate the use of hydrogen on rotorcraft and indentify the key issues for the actual development, manufacturing and installation of all the components, for instance lofting of large hydrogen tanks, flight performance estimation and costs.

A feasible solution is sought here by casting this question as an optimization problem, by establishing an appropriate objective function to be minimized under relevant constraints. The objective function is represented by the total weight related to the powertrain. The constraints reflect aircraft requirements, battery limitations, FC operational modes as well as technology specifications.

The formulation is cast as a constrained non linear optimization problem, where non linear equality and inequality constraints are involved. This is applied to a specific design flight mission, which is simulated in time through embedded rotorcraft flight mechanics equations, in case a detailed flight record (i.e., altitude, true airspeed, vertical airspeed and required power) is not available. The final solution provides the optimal values of the power share among battery and FC during the design mission, resulting in an optimal value of the hydrogen, hydrogen tank, battery, FC and Electric Motor (EM) masses, as well as an additional mass toll deriving from cables, thermal management system, and drivetrain.

The methodology has been implemented in an original algorithm, HERACLES, depicted in Figure 1. Starting from an input file which contains all the necessary data (i.e. aircraft specifications, drivetrain properties and mission profile) a pre-sizing tool [14] estimates an initial guess for the optimization vector ($\boldsymbol{x}$), which contains all the variables to compute the cost function and the constraints:

$$\boldsymbol{x} = \left[\frac{M_B}{M_0}, \frac{M_{FC}}{M_0}, \frac{M_{H_2}}{M_0}, \frac{M_T}{M_0}, \frac{M_{EM}}{M_0}, \frac{M_{TMS}}{M_0}, \right. \\ \left. \frac{M_{GB}}{M_0}, \frac{M_C}{M_0}, \frac{\tau_{EM}}{\tau_0}, \frac{\Omega_{EM}}{\Omega_0}, \frac{\boldsymbol{P}_B}{P_0}, \frac{\boldsymbol{P}_{FC}}{P_0} \right] \tag{1}$$

The symbols M_B, M_{FC}, M_{H_2}, M_T, M_{EM}, M_{TMS}, M_{GB}, M_C represent the battery, FC, hydrogen, tank, EMs, Thermal Management System (TMS), gearbox and cables mass respectively. On the other hand, the vectors $\boldsymbol{P}_B$ and $\boldsymbol{P}_{FC}$ are used for the description of the battery and fuel cell power histories during the flight mission which is sampled in an arbitrary amount of time steps (N). As regards the EMs power, it has been split into torque τ_{EM}, and rotational speed Ω_{EM}, in order to optimize both. All the variables have been normalized by four factors computed through the pre-sizing loop, i.e. a reference mass M_0, torque τ_0, rotational speed Ω_0 and power P_0. The vector of variables $\boldsymbol{x}$ is then used to compute the cost function $J(\boldsymbol{x})$, which is the normalized total mass of the powertrain:

$$J(\boldsymbol{x}) = \frac{n_B M_B + n_{FC} M_{FC} + M_{H_2}}{M_0} + \\ + \frac{M_T + M_{EM} + M_{GB} + M_{TMS} + M_C}{M_0} \tag{2}$$

The cost function takes into account the presence of n_B battery packs and n_{FC} FC modules.

Referring at Figure 1, after the cost function is computed, the design mission is simulated. The mission simulation phase embodies suitable physical models for the estimation of FC and battery performance in order to evaluate the quantity of consumed hydrogen mass and battery energy. Then the solution is evaluated to ensure its feasibility. In particular, the

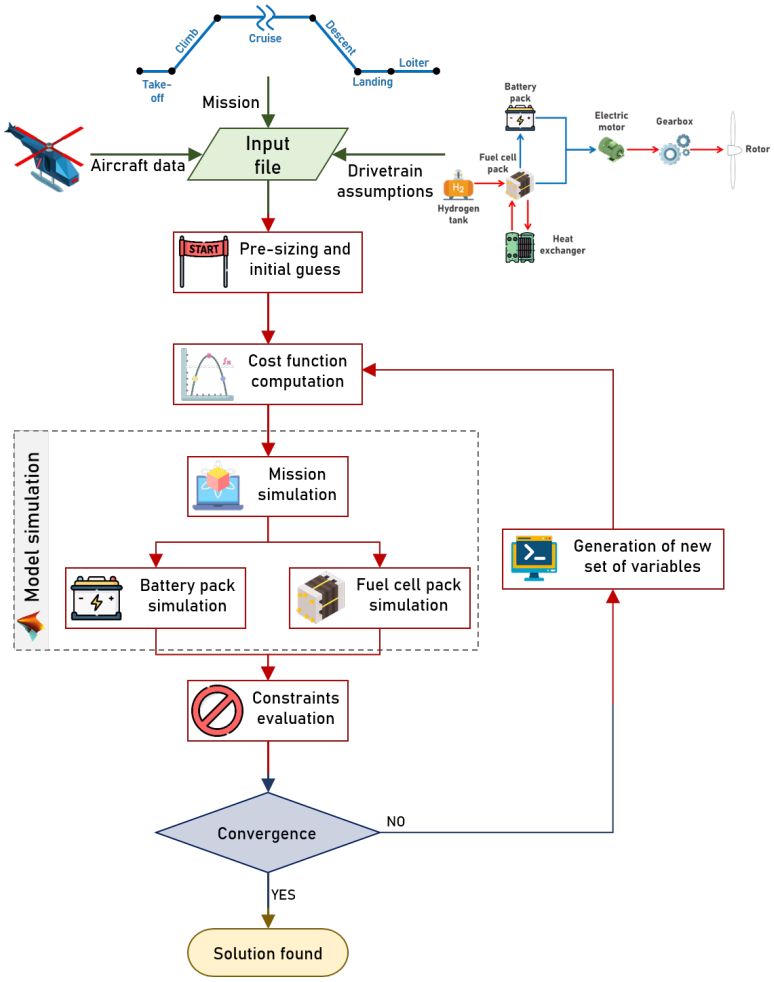

Figure 1: Flowchart of the HERACLES algorithm.

parameters influencing the components of the cost function need to satisfy an array of constraints, which reflect both technological limits and models of the powertrain dynamics and aircraft flight mechanics. These constraints can be formalized as a set of 18 relations: 1 equality and 17 inequalities. The equality is used to ensure that, throughout the mission, the total power generated by the FC and battery modules matches the rotor mechanical power requested by the aircraft, considering also the drivetrain and electrical distribution efficiencies. At the same time, the inequalities account for a variety of physical and operational limitations of the aircraft and the powertrain components, including limits to battery SoC for the sake of the cells safety and longevity, and emergency flight phases, such as OEI conditions. Additional inequality constraints are used to size the masses of the powertrain components in Equation (2), recurring to the same physical and statistical models used in [14].

In particular, the FC packs are sized with either the maximum power or the maximum efficiency point at a fixed maximum voltage as design point. The current, FC efficiency, and effective FC power are then calculated at each time step using the polarization curve.

The battery pack is simulated through a high-fidelity dynamic model which permits to evaluate the power limits and the SoC at each time step [15].

The hydrogen tank mass is sized using a gravimetric index.

The EMs are sized according to their specific torque and power characteristics [16].

The TMS and gearbox masses, are calculated using state-of-art regressions [16], [17].

The electrical power distribution system is sized accordingly a cable weight model for aeronautical applications taken from [18].

Finally, after that the constraints are evaluated, the algorithm compares the feasibility and the first order optimally with respect to a predetermined target. Therefore, upon convergence, the methodology returns the optimal values of all the powertrain component masses (i.e., FCs, battery pack, liquid hydrogen, tank, EMs, cables, driveshaft, and TMS), as well as defin-

Table 1: Technology assumptions for the TEH-R study case.

Component	Description	Value	M.U.
Electric motors	No. of EM	2	
	Type	axial flux	
	RPM range	$[237 \div 6,000]$	RPM
	Overrating	1.25	
Battery	No. of packs	2	
	Specific energy (pack level)	215	Wh/kg
	Continuous (peak) discharge C-rate	12 (23)	-
	Energy density	430	Wh/m^3
Fuel cell system	No. of stacks	2	
	Specific power (including BoP except TMS)	2.133	kW/kg
	Operating temperature	353	K
	Operating pressure	1.5	bar
	Cell area	200	cm^2
	Compressor efficiency	0.8	-
Other parameters	DC-bus voltage	1000	V
	Cryogenic tank gravimetric index	50	%

ing an optimal usage spectrum for both power sources.

It is worth noting that, the physical models behind each subsystem of the methodology, make it suitable to work on a series of similar optimization problems linked to aircraft design and flight performance estimation. For instance, Equation (2) can be changed in order to minimize other relevant design parameters, such as fuel consumption, battery life, or direct operating costs. Additionally, by freezing a specific powertrain solution sized during a preliminary design phase, it is possible to simulate off-design conditions, such as different mission profiles and identify the best power vectors ($\boldsymbol{P}_B$ and $\boldsymbol{P}_{FC}$) to minimize arbitrary cost functions.

HERACLES has been coded in MATLAB® and solves the minimization problem using the embedded optimization toolbox with either the `fmincon` constrained optimization function or with `ga` which finds minimum using genetic algorithm.

3 CASE STUDY

After checking the proper behaviour of the algorithm through trivial solutions (i.e., high mass of battery cell or FC), the optimal procedure was applied to the retrofit of the Clean Sky Green Rotorcraft Twin Engine Heavy Helicopter – 2020 Reference (TEH-R), a heavy category (MTOW$\geq$8 ton) helicopter with a takeoff power in the range of 2 MW. TEH-R was chosen because it represents the current state of the art in rotorcraft technology, allowing the benefits of a fleet substitution rate to be estimated, its data are partly available in [19].

Therefore, the scope of the analysis is to replace the conventional Thermal Engine (TE)-driven powertrain of the TEH-R with a hydrogen-driven powertrain featuring a FC system. A schematic of the considered series powertrain architecture is portrayed in Figure 2.

The retrofit solution is envisioned within a 2030 time frame. Input parameters about technological assumptions (i.e. battery and FC performance, tank gravimetric index and EM properties) are instead considered for the year 2025, allowing a 5 year gap for certification and testing. Data are summarised in Table 1. The FC specific power indicated in the table considers also the Balance of Plant (BoP) (compressor, humidifier) without the cooling system, accounted for separately [20]. Concerning the cryogenic tank, the gravimetric index is assumed equal to 50%. This value is considered conservative with respect to the values reported by [21]. The EMs are considered to be of the axial flux typology and the rotational speed can range from the main rotor speed to a maximum value of 6,000 RPM, other considerations have been derived from previous experiences on a electric tail rotor application [22]. Finally, the battery specific energy and C-rate values are based on state-of-the art power specialized Li-ion cells [23]–[25] assuming about 3% of annual improvement with respect to the actual values.

4 RESULTS

4.1 The optimal results

As depicted in Figure 3 HERACLES returns a weight breakdown of the retrofitted solution, splitting the MTOW among the powertrain components introduced in Equation (1). In the component-by-component

weight breakdown of Figure 3a the purple bar indicates the mass of the non-propulsive elements, i.e. structure, landing gear, avionics, and other non-propulsive systems, whose contribution amounts to the one of the original TEH-R. Figure 3b groups the weight contribution into payload weight, empty weight and fuel weight, and compares the overall amounts with TEH-R (empty blue rectangles). It is possible to notice a reduction of the fuel weight of the retrofitted machine with respect to the original values of TEH-R. However, the 1,484 kg (-84.6%) of less fuel is counterbalanced by the increasing empty fraction of 1,807 kg (+35.9%). This reduces the residual payload by 323 kg (-11.9%).

The hydrogen tank is capable of hosting 271 kg of liquid hydrogen. According to Winnefeld's model [21], the considered gravimetric index implies a thickness of 200 mm that allows for a self-emptying time of 1.4%/h at standstill in ISA+35 and steady-state conditions.

The time histories depicted in Figure 4a show the optimal power management strategy of FC and battery outputs. In particular, the sum of the battery power (blue line) and FC power (orange line), net of the EMs, power electronics and driving system efficiencies must match the required power (green line). The dashed black line represents the mission profile in terms of altitude.

The corresponding tank level (yellow line), battery SoC (blue line) and FC throttle (orange line) are shown in Figure 4b. The SoC of the battery pack is always contained between a maximum and a minimum value respectively equal to 90% and 10%. In this case, the dashed-dotted black line represents the mission profile in terms of range.

From the time histories of Figures 4a and 4b it is possible to observe that the optimal usage of the battery pack, resulting from the algorithm, consists in depleting the charge mainly during peak phases (takeoff) and residually discharging during cruise. Towards the end of the mission, the battery is charged again to provide the power boost necessary for landing. Then, some residual recharge happens to avoid getting below the minimum 10% SoC.

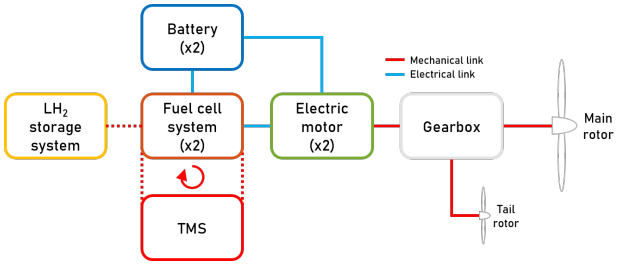

Figure 2: Schematic of the fuel cell-based hydrogen-powered powertrain.

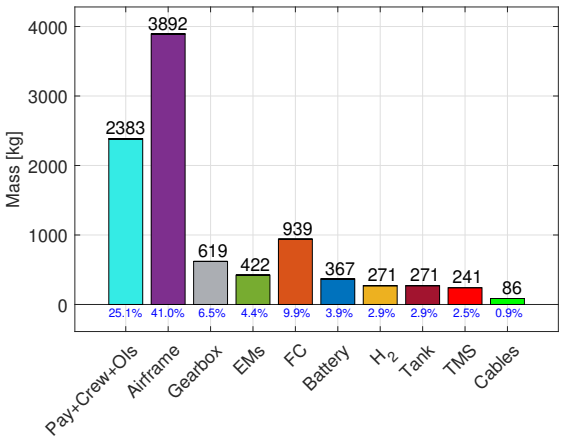

(a) Component-by-component weight breakdown.

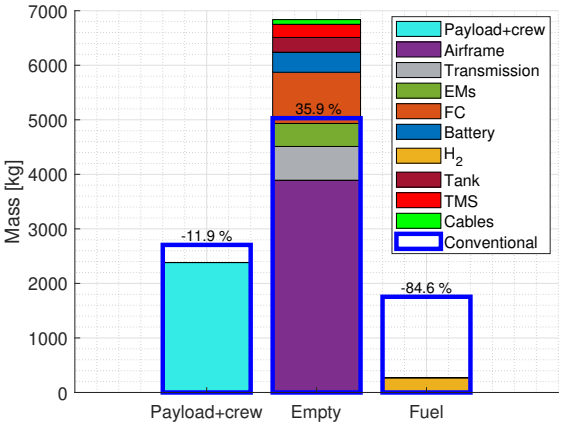

(b) Comparison between the retrofit solution and the original aircraft.

Figure 3: Results of the TEH-R solution.

Figure 4c shows FC efficiency along the mission, obtained matching the power requirement with FC polarization curve at each time step.

Figure 4d depicts battery power (blue line) within its upper and lower bounds, which are a function of the battery SoC. These limits are widened during transients phases (corresponding to takeoff and landing) where the battery power can use a boost power mode.

In Table 2 are listed some of the most important outputs of the algorithm, such as, the rated powers of EMs, battery pack and FC, the sizing of the cryogenic tank and the volumes of these subsystems.

Finally, in Figure 5 is shown the lofting of the powertrain subsystems for the retrofitted solution.

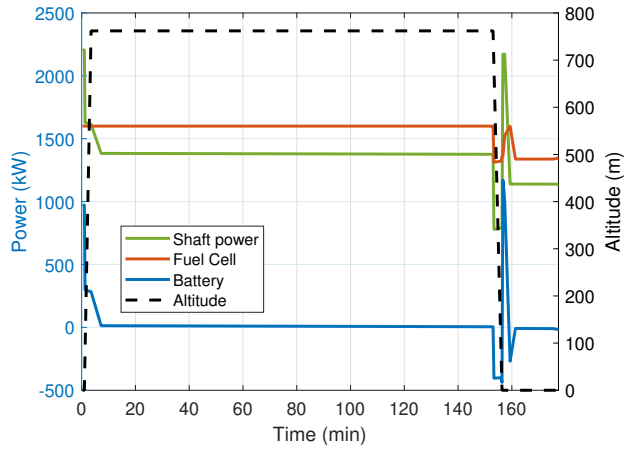

(a) Power usage along the mission profile.

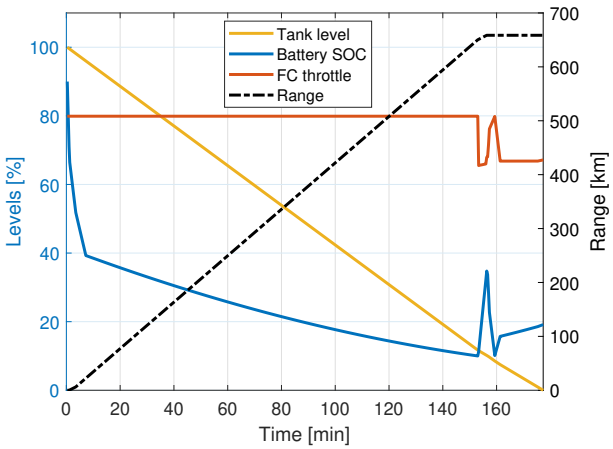

(b) Power usage along the mission profile.

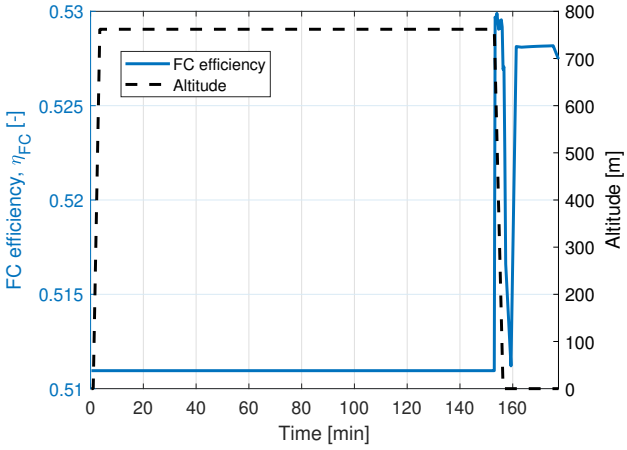

(c) FC efficiency.

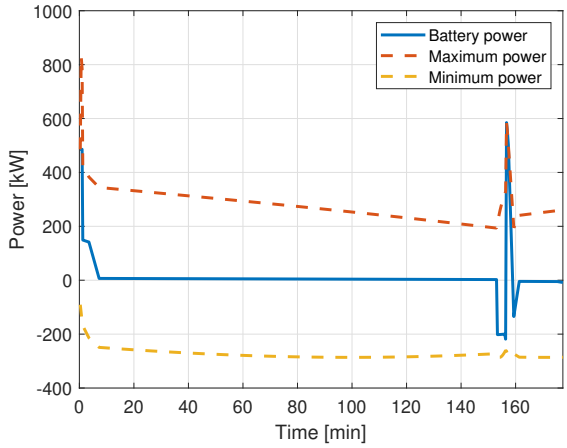

(d) Battery power profile compared to the computed power limits.

Figure 4: Optimized powertrain results.

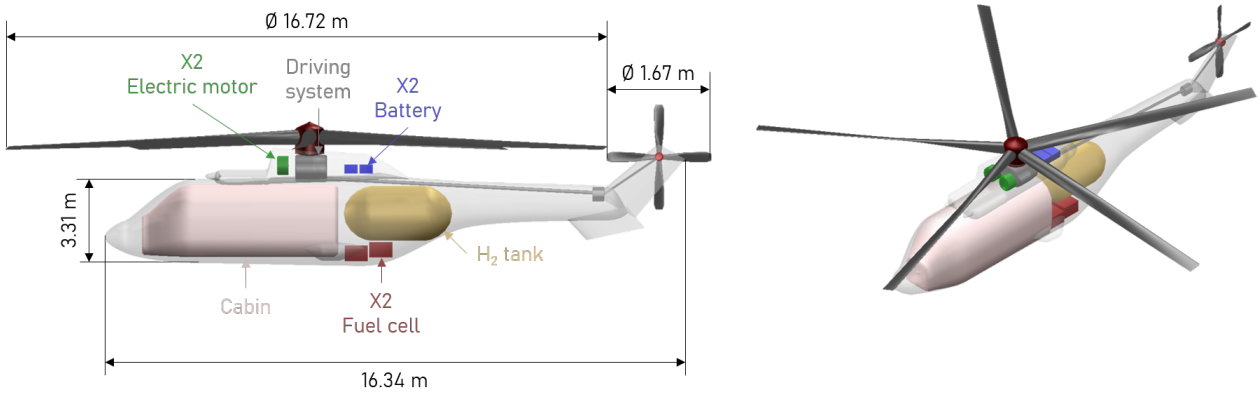

Figure 5: Rotorcraft dimensions and powertrain components lofting.

4.2 First guess and optimized solution comparison

To better visualize the effectiveness of the optimization loop and understand how it can reduce the overall powertrain weight, a comparison between the optimization results, already discussed in Section 4.1, and the algorithm first guess, is shown in Figure 6. The initial guess derives from a pre-sizing

Table 2: Results of the HERACLES sizing process for TEH-R FC-powered solution.

Component	**Description**	**Value**	**M.U.**
Electric motors	MCP (Peak power)	1,001.0 (1,251.3)	kW
	Weight	211.0	kg
	Diameter	0.52	m
	Length	0.29	m
	Speed	6,000	RPM
Battery	No. of cells (s x p)	269 x 6	
	MCP (Peak power)	460 (828)	kW
	Nominal energy	39.58	kWh
	Weight	183.5	kg
	Volume	0.0635	m^3
Fuel cell system	No. of cells (s x p)	1,277 x 6	
	Power	1,001	kW
	Weight	469.5	kg
	Volume	0.3613	m^3
Hydrogen Tank	Diameter	1.51	m
	Total length (including end caps)	3.01	m
	External Volume	4.47	m^3
	Boil-off rate	1.4	%/h
Transmission	Gear ratio	25.32	
	Weight	619.1	kg
Cabling	Overall length	32.5	m
	Weight	86.1	kg

tool, namely Retrofit Of HydroGen powEred Rotorcraft (ROHGER), which is described in [14]. Hence, Figure 6a depicts the difference in powertrain weights between HERACLES and ROHGER results. Here, it is possible to see a payload increase of 236 kg, which is approximately equal to 9% of the MTOW. This increase in payload is due to a reduction in the overall empty weight, which can be explained component by component as follows:

- EMs: the optimization algorithm converges to a higher rotational speed of the electric motors, specifically equals to 6,000 RPM, against to the 2,000 RPM of the first guess. Thus, at constant specific torque and required power, the electric machine weight is reduced regardless of inverter mass [16], saving a total of 82 kg for each EM.
- Gearbox: because of the higher gear ratio of the gearbox due to the rotational speed of the EMs, its weight increases by 24 kg, which is a very small price to pay given the high sparing weight obtained for the EMs.
- FCs: better battery utilization, as shown in Figure 6b, allows for a FC power reduction which results in a lower weight of approximately 134 kg while maintaining OEI powers.
- Battery: HERACLES aims for a small increase in battery pack weight of 12 kg for an optimal hybridization factor of around 32% compared to the initial value of 29%; where the hybridization factor is computed through the battery and fuel cell maximum continuous rated powers as follows:

$$\phi = \frac{P_B}{P_B + P_{FC}} \tag{3}$$

- Hydrogen: the fuel mass is lower for two reasons, first, the better power usage of the two energy sources allows the FC to operate at a higher efficiency throughout the mission, and second, the pre-sizing ROHGER algorithm accounts for the boil-off rate, specifically 13.1 kg of vented hydrogen during a 30 minute ground hold phase, neglected for simplicity during the optimization.
- Hydrogen tank: whether a 50% of gravimetric index has been considered in the optimization algorithm, through ROHGER the tank is effectively sized showing that a gravimetric index of 61.2%, including BoP, can be reached, so that 50% is instead a conservative value.
- TMS: due to the lower power of the FC stack, 15 kg of TMS weight can be saved.
- Cables: the total amount of electrical power is constant, even if it is split differently between FC and battery, so the amount of cable weight does not change.

Finally, Figure 6b depicts the best power usage of the FCs and battery packs discovered by HERACLES

in comparison to the initial guess. It is clear that the battery pack's ability to reduce the power peak of the FCs allows for a lighter solution.

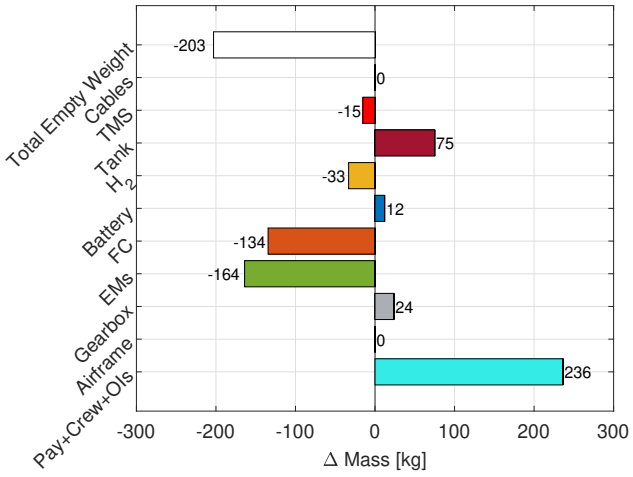

(a) Mass breakdown comparison.

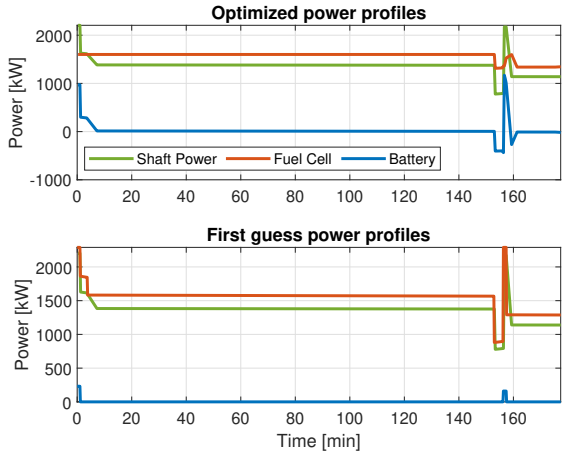

(b) Power profiles comparison.

Figure 6: Comparison between the oprimized solution and the first guess.

4.3 Sensitivity analysis

Some sensitivity studies on the design parameters of the main powetrain components are here presented.

In particular, Figure 7 shows how the percentage difference in payload between the retrofitted machine and the original TEH-R changes with respect to the FC specific power and tank gravimetric index. Given that the fuel is the energetic content of the hydrogen system and that its specific energy is constant, the variation of the tank weight represents the system's specific energy. As a result, it is possible to overall observe the hyperbolic behaviour of the payload contour line with varying tank gravimetric index (y axis) and FC specific power (x axis).

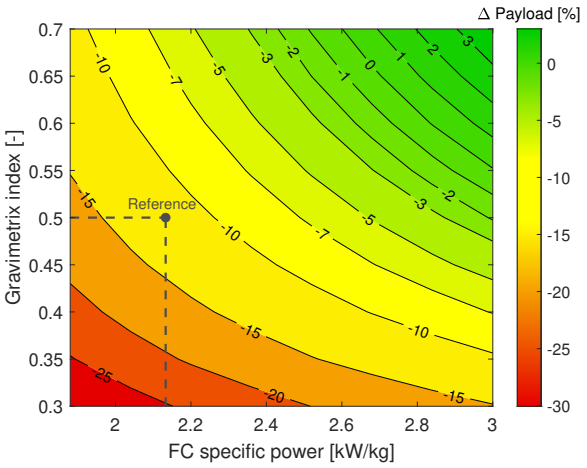

Figure 7: Payload of the retrofitted solution with respect to FC specific power and tank gravimetric index.

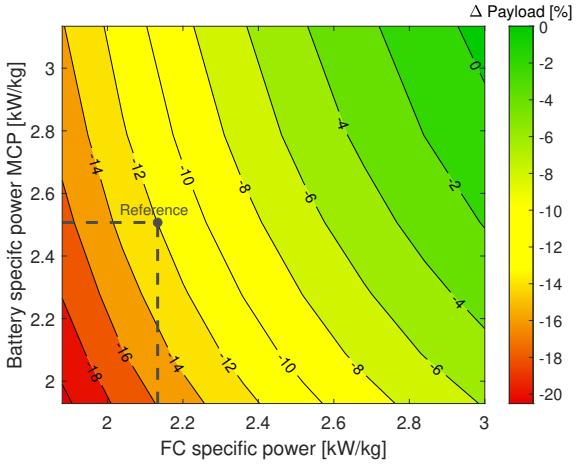

Figure 8: Payload variation of the retrofitted solution with respect to FC and battery specific power.

Looking at the solution's sensitivity to both power sources, Figure 8 depicts the payload variation against the battery (y-axis) and FC (x-axis) specific power. The contour lines are flattened on the abscissa axis due to the high weight of the FC, which means that the payload is more sensitive to variations in the specific power of the latter than to those of the battery.

Analogously to Figure 8, Figure 9 shows the sensitivity of the resulting optimal hybridization factor ϕ to the same variables, i.e. FC and battery specific power. It is clear from the graph, that the value of the hybridization factor remains almost constant despite the changes in the two variables. A constant ϕ means that the ratio between battery and FC power does not vary since HERACLES converges always to the same power share. The reasons of this behaviour are probably due to the values of the battery peak specific power, always higher than the one of the FC,

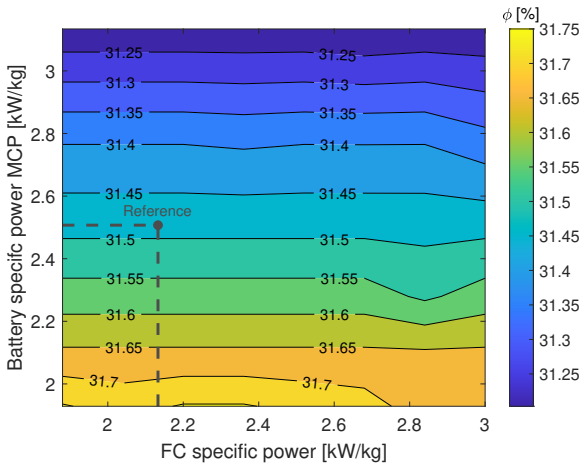

Figure 9: Hybridization factor with respect to FC and battery specific power.

and mainly to the particular aircraft and design flight mission characteristics. In particular the parameter leading the optimal ϕ is represented by the difference between the takeoff and the cruise power, divided by the takeoff power.

5 CONCLUSION

In this paper, a methodology for the optimal retrofit of a hydrogen-powered VTOL is presented. The sizing is based on an original tool, HERACLES, that implements a constrained optimization problem to size the powertrain components (i.e., battery, FCs, hydrogen, tank, gearbox, EMs, TMSs and cables) and returns the optimal power share over a pre-defined mission profile.

The algorithm is capable of addressing multiple rotorcraft categories, from lightweight single engine to fast compound architectures. The proposed solution is compliant with the airframe of the considered reference aircraft, since it preserves the MTOW. In particular, the results presented refer to the TEH-R case of study, or a large rotorcraft FC-based retrofit. Due to an increment of the empty weight because of the FC system, the cryogenic tank and EMs, the overall residual payload is 11.9%, lower than the original aircraft. This can be seen as the price to pay, for the present study case, to obtain the result of zero CO_2 emissions with today's technology. However, comparing the results to the first guess an increment of 9% of the payload is possible optimizing the architecture hybridization factor, the usage of the battery pack and the FCs, and increasing the EMs rotational speed. The results are highly correlated to the state-of-the-art technology, with particular emphasis on the payload's dependence on assumptions about FCs, batteries, and tank gravimetric index. The sensitivity analysis also indicates the improvements that must be made to FC and battery technologies for a given retrofit solution in order to be applicable without penalization in terms of payload and range.

The flexibility of the developed methodology lends itself to be applied on various platforms with different architectures; this allows to evaluate different technological solutions, indicating when they could be ready to sustain profitable business cases in the future. Further applications of HERACLES will be targeted to understand which combination of propulsion technology and powertrain could be successful to maximize performance while pursuing the restrictive carbon reduction goals of the aviation sector.

REFERENCE

[1] L. A. Garrow, B. J. German, and C. E. Leonard, "Urban air mobility: A comprehensive review and comparative analysis with autonomous and electric ground transportation for informing future research," *Transportation Research Part C: Emerging Technologies*, vol. 132, p. 103 377, 2021, ISSN: 0968-090X. DOI: https://doi.org/10.1016/j.trc.2021.103377.

[2] *Electric vtol news™, 2020. evtol aircraft directory.* https://evtol.news/aircraft, Accessed: February 22nd, 2022.

[3] N. Polaczyk, E. Trombino, P. Wei, and M. Mitici, "A review of current technology and research in urban on-demand air mobility applications," English, in *8th Biennial Autonomous VTOL Technical Meeting and 6th Annual Electric VTOL Symposium 2019*, Vertical Flight Society, 2019, pp. 333–343.

[4] A. Datta and W. Johnson, "Powerplant design and performance analysis of a manned all-electric helicopter," *Journal of Propulsion and Power*, vol. 30, pp. 490–505, Mar. 2014. DOI: 10.2514/1.B34843.

[5] N. Lapeña-Rey, J. Mosquera, E. Bataller, and F. Ortí, "First fuel-cell manned aircraft," *Journal of Aircraft*, vol. 47, no. 6, pp. 1825–1835, 2010. DOI: 10.2514/1.42234.

[6] J. Kallo, S. Flade, T. Stephan, and J. Schirmer, "Antares dlr h2 - test bed for electric propulsion," in *53rd AIAA Aerospace Sciences Meeting*. DOI: 10.2514/6.2015-1305. eprint: https://arc.aiaa.org/doi/pdf/10.2514/6.2015-1305.

[7] A. L. d. Castro, P. T. Lacava, and C. H. B. Mourão, "Feasibility of using fuel cell in a small aircraft," in *AIAA AVIATION 2021 FORUM*. DOI: 10.2514/6.2021-3189.

[8] Y. Khan, A. Rolando, F. Salucci, C. Riboldi, and L. Trainelli, "Hybrid-electric and hydrogen powertrain modelling for airplane performance analysis and sizing," in *IOP Conference Series: Materials Science and Engineering*, IOP Publishing, vol. 1226, 2022, p. 012 071.

[9] W. Ng and A. Datta, "Hydrogen fuel cells and batteries for electric-vertical takeoff and landing aircraft," *Journal of Aircraft*, vol. 56, no. 5, pp. 1765–1782, 2019. DOI: 10.2514/1.C035218.

[10] W. Ng, M. Patil, and A. Datta, "Hydrogen fuel cell and battery hybrid architecture for range extension of electric vtol (evtol) aircraft," *Journal of the American Helicopter Society*, 2021.

[11] Y. Xie, A. Savvarisal, A. Tsourdos, D. Zhang, and J. Gu, "Review of hybrid electric powered aircraft, its conceptual design and energy management methodologies," *Chinese Journal of Aeronautics*, vol. 34, no. 4, pp. 432–450, 2021, ISSN: 1000-9361. DOI: https://doi.org/10.1016/j.cja.2020.07.017.

[12] M. A. Rendón, C. D. Sánchez R., J. Gallo M., and A. H. Anzai, "Aircraft hybrid-electric propulsion: Development trends, challenges and opportunities," *Journal of Control, Automation and Electrical Systems*, vol. 32, no. 5, pp. 1244–1268, Oct. 2021, ISSN: 2195-3899. DOI: 10.1007/s40313-021-00740-x.

[13] T. Lei, Z. Yang, Z. Lin, and X. Zhang, "State of art on energy management strategy for hybrid-powered unmanned aerial vehicle," *Chinese Journal of Aeronautics*, vol. 32, no. 6, pp. 1488–1503, 2019, ISSN: 1000-9361. DOI: https://doi.org/10.1016/j.cja.2019.03.013.

[14] F. Salucci, A. Nesci, G. Vicenzotti, and M. Brunetti, "Retrofit of hydrogen-powered helicopters: A sizing approach," in *AIAA AVIATION 2022 Forum*. DOI: 10.2514/6.2022-3206.

[15] G. L. Plett, *Battery Management Systems, Volume II: Equivalent-Circuit Methods*. Artech House, 2015.

[16] W. Johnson, *NDARC, NASA Design and Analysis of Rotorcraft*. Ames Research Center, 2015.

[17] J. W. Chapman, S. L. Schnulo, and M. P. Nitzsche, "Development of a thermal management system for electrified aircraft," in *AIAA Scitech 2020 Forum*. DOI: 10.2514/6.2020-0545.

[18] S. Stückl, "Methods for the design and evaluation of future aircraft concepts utilizing electric propulsion systems," Ph.D. dissertation, Technische Universität München, 2016.

[19] J. Stevens, C. Smith, V. Pachidis, L. Thevenot, and R. D'Ippolito, "Cleansky green rotorcraft noise and emissions benefits–maximizing the impact of new technologies," 2015.

[20] F. Salucci, "Design of electric-powered aircraft for commercial transportation," en, Doctoral dissertation, Politecnico di Milano, Milan, May 2021.

[21] C. Winnefeld, T. Kadyk, B. Bensmann, U. Krewer, and R. Hanke-Rauschenbach, "Modelling and Designing Cryogenic Hydrogen Tanks for Future Aircraft Applications," en, *Energies*, vol. 11, no. 1, p. 105, Jan. 2018, ISSN: 1996-1073. DOI: 10.3390/en11010105.

[22] K. Stickels, M. Brunetti, M. Barber, *et al.*, "Advances in helicopter electric tail rotor drive," 2017.

[23] J. Rohacs and D. Rohacs, "Energy coefficients for comparison of aircraft supported by different propulsion systems," *Energy*, vol. 191, p. 116 391, 2020, ISSN: 0360-5442. DOI: https://doi.org/10.1016/j.energy.2019.116391.

[24] G. E. Blomgren, "The development and future of lithium ion batteries," *Journal of The Electrochemical Society*, vol. 164, no. 1, A5019–A5025, Dec. 2016. DOI: 10.1149/2.0251701jes.

[25] *Roadmap on mobile applications of batteries*. Batteries Europe Working Group 5 European Commission, 2021.

[26] C. Spiegel, *PEM Fuel Cell Modeling and Simulation Using Matlab*. May 2008. DOI: 10.1016/B978-0-12-374259-9.X5001-0.